

1 Pulsed broad-spectrum UV light effectively inactivates SARS-CoV-2 on multiple surfaces

2 Alexander S. Jureka, Caroline G. Williams, and Christopher F. Basler\*

3 Center for Microbial Pathogenesis, Institute for Biomedical Sciences, Georgia State University,

4 Atlanta, GA, 30303

5 \*Corresponding Author

6 Center for Microbial Pathogenesis

7 Institute for Biomedical Sciences

8 Georgia State University

9 Atlanta, GA 30303

10 Tel. (404) 413-3651

11 Email: [cbasler@gsu.edu](mailto:cbasler@gsu.edu)

12

## 13 **Abstract**

14 The ongoing SARS-CoV-2 pandemic has resulted in an increased need for technologies capable  
15 of efficiently disinfecting public spaces as well as personal protective equipment. UV light  
16 disinfection is a well-established method for inactivating respiratory viruses. Here, we have  
17 determined that broad-spectrum, pulsed UV light is effective at inactivating SARS-CoV-2 on  
18 multiple surfaces. For hard, non-porous surfaces we observed that SARS-CoV-2 was inactivated  
19 to undetectable levels on plastic and glass with a UV dose of 34.9 mJ/cm<sup>2</sup> and stainless steel with  
20 a dose of 52.5 mJ/cm<sup>2</sup>. We also observed that broad-spectrum, pulsed UV light is effective at  
21 reducing SARS-CoV-2 on N95 respirator material to undetectable levels with a dose of 103  
22 mJ/cm<sup>2</sup>. We included UV dosimeter cards that provide a colorimetric readout of UV dose and  
23 demonstrated their utility as a means to confirm desired levels of exposure were reached.  
24 Together, the results present here demonstrate that broad-spectrum, pulsed UV light is an  
25 effective technology for the inactivation of SARS-CoV-2 on multiple surfaces.

26

## 27 **Introduction**

28 In late 2019, the novel severe acute respiratory distress syndrome virus 2 (SARS-CoV-2)  
29 emerged from Wuhan, China [1,2]. SARS-CoV-2 is a member of the *Coronaviridae* family of  
30 enveloped negative-sense RNA viruses. It is classified in the *Betacoronavirus* genus of which  
31 other notable members are the highly pathogenic SARS-CoV and the Middle East respiratory  
32 syndrome virus (MERS-CoV) [3]. Since its emergence, SARS-CoV-2 has been the cause of the  
33 most severe pandemic in the last century. Despite significant efforts to contain the spread of  
34 SARS-CoV-2, as of February 7<sup>th</sup>, 2021 it has caused over 105 million cases and resulted in over  
35 2.3 million deaths worldwide [4].

36

37 High case counts raise concerns about infections arising from contaminated public spaces, such  
38 as mass transit vehicles and hospital spaces that have housed SARS-CoV-2 positive patients.  
39 The need for effective means to eliminate SARS-CoV-2 from environmental surfaces is supported  
40 by studies demonstrating the capacity of the virus to survive on a variety of surfaces for significant  
41 periods of time on a variety of surfaces. For example, infectious virus could be recovered from  
42 plastic or steel for 72 hours and on cardboard after 24 hours [5]. There is also substantial evidence  
43 that SARS-CoV-2-infected individuals shed virus into their environment. Analysis by RT-PCR of  
44 COVID-19 patient rooms and other hospital settings demonstrated frequent contaminating viral  
45 RNA on surfaces [6-9]. In some studies, however, lower frequency of surface contamination has  
46 been reported [10]. Outside of the healthcare setting, rooms of cruise ship passengers who had  
47 COVID-19 were also contaminated with viral RNA [11]. Viral RNA has also been found on various  
48 surfaces in households with SARS-CoV-2 infected individuals [12,13].

49  
50 Given the potential for fomite transmission, the World Health Organization has provided guidance  
51 on cleaning and disinfection where SARS-CoV-2 contamination could occur [14]. Because of the  
52 importance of respiratory protection and shortages of personal protective equipment, methods to  
53 disinfect and reuse N95 filtering respirators has also been of significant interest [15,16]. UV light  
54 as well as other methods have been either proposed or tested as a means to disinfect N95 masks  
55 and other PPE [16-24].

56  
57 While chemical disinfectants and alcohols are effective methods of inactivating SARS-CoV-2 in  
58 most circumstances, disinfection of large spaces using these methods is a laborious process  
59 requiring close contact with potentially contaminated surfaces [25-28]. UV light has long been  
60 established as an effective and direct method for the inactivation of enveloped viruses [29]. UV  
61 disinfection approaches provide a significant advantage as they are less laborious to employ and  
62 do not necessarily require close contact with potentially contaminated surfaces.

63

64 Here, we report the efficacy of broad-spectrum, pulsed UV light in inactivating SARS-CoV-2 on  
65 glass, plastic, stainless steel, and N95 respirator material. Additionally, we have tested the  
66 effectiveness of UV dosimeter cards that would provide end users the ability to quickly determine  
67 if a high enough dosage of UV light has been applied to a surface. Together, the data reported  
68 here demonstrate that broad-spectrum, pulsed UV light is highly effective at inactivating SARS-  
69 CoV-2 on multiple surfaces.

70

## 71 **Materials and Methods**

### 72 Cells and virus

73 Vero E6 cells (ATCC# CRL-1586) were maintained in DMEM supplemented with heat-inactivated  
74 fetal bovine serum (FBS; Gibco). SARS-CoV-2, isolate USA\_WA1/2020, was obtained from the  
75 World Reference Collection for Emerging Viruses and Arboviruses at the University of Texas  
76 Medical Branch. SARS-CoV-2 virus stocks were propagated as previously described [30].

### 77 Surface Inoculation

78 The following surfaces were tested within the wells of a 24 well plate in triplicate: glass coverslips,  
79 0.5x0.5 cm stainless steel squares, the tissue culture plate well (plastic; polystyrene), and 0.5x0.5  
80 cm squares of N95 respirator material from a 3M™ 9210+ respirator. Four 0.5x0.5 cm squares of  
81 UV dosimeter cards (Intelligo Technologies) were placed in each corner of the plate to confirm  
82 even UV exposure across the plates and allow comparison of the cards to a UV dosage meter as  
83 a means to quantify exposure dose (Supplemental Figure 1). For surface inoculation, 12  $\mu$ L of  
84 SARS-CoV-2 stock virus (USA\_WA1/2020;  $8.3 \times 10^4$  pfu) in OptiMEM supplemented with 1x  
85 antibiotic/antimycotic (Gibco) was pipetted directly onto each surface being tested and spread  
86 with a pipette tip to facilitate efficient drying. Surface samples inoculated with virus were allowed  
87 to dry in the 24 well plates with the lids off for 1 hour at room temperature in the biosafety cabinet.  
88 After the surfaces had dried, the 24-well plate lids were replaced, and all plates not being exposed

89 to UV were placed inside a black opaque container in a separate biosafety cabinet to avoid  
90 incidental UV exposure.

#### 91 UV exposures

92 The Puro UV Helo F2 device was placed in the center of the biosafety cabinet. The test samples  
93 as well as an UV dosage meter (ILT2500; International Light Technologies) equipped with a  
94 calibrated SED270 detector were placed 1 meter away facing the Helo F2 device. Care was taken  
95 to ensure that the UV dosage meter and surfaces being exposed were as inline as possible before  
96 beginning testing. The 24-well plates containing the test surfaces were positioned so that the  
97 plates were nearly vertical (~85 degrees) and approximately 3 inches above the surface of the  
98 biosafety cabinet to avoid shadowing (Supplemental Figure 2). Once the 24-well plate was  
99 positioned, the UV dosage meter was zeroed to account for ambient UV. Once zeroed, the UV  
100 dosage meter was set to “integrate” mode to measure UV dosage over time and total pulse-  
101 counts. The Helo F2 device was initiated using an electronic timer set to the indicated exposure  
102 time with an additional minute added to account for device startup procedures. UV dosage for a  
103 given timepoint was recorded as mJ/cm<sup>2</sup> along with the corresponding pulse-count. UV dosimeter  
104 cards were collected and photographed to record the color change. One card from the 3-minute  
105 timepoint was lost due to airflow in the biosafety cabinet. For the purposes of graphical depiction,  
106 UV dosimeter card color post-UV exposure was replicated using the eyedropper tool in Adobe  
107 Illustrator.

#### 108 Sample harvesting

109 After all exposures were complete, 1 mL of sterile PBS was placed inside the surface-containing  
110 wells and allowed to rehydrate for 15 minutes before transferring to a 1.5 mL centrifuge tube and  
111 storing at -80C for further analysis. Additionally, 12 µL of stock virus (USA\_WA1/2020; 8.3x10<sup>4</sup>  
112 pfu) was added to 1 mL of sterile PBS and stored at -80C at the same time as the other samples  
113 in order to control for the loss of virus titer due to the drying process.

#### 114 Virus quantification by plaque assay

115 Vero E6 cells were plated to confluency in 24-well plates 24 hours prior to infection. Ten-fold serial  
116 dilutions of SARS-CoV-2 containing samples were added onto the cells (100  $\mu$ L) and virus was  
117 adsorbed for 1 hour with shaking at 15-minute intervals. After the adsorption period, 1 mL of 0.6%  
118 microcrystalline cellulose in DMEM supplemented with 2% fetal bovine serum and 1x antibiotic-  
119 antimycotic was overlaid onto to the cells and plates were incubated at 37C/5% CO<sub>2</sub> for 72 hours,  
120 as described previously [30]. After incubation, the microcrystalline cellulose overlay was aspirated  
121 from the well, and cells were fixed with 10% neutral buffered formalin for 1 hour at room  
122 temperature. Plates were then washed with water and stained with crystal violet to visualize  
123 plaques. Plaques were quantified and recorded as plaque forming units per mL (pfu/mL). All  
124 samples assayed were only subjected to one freeze-thaw cycle.

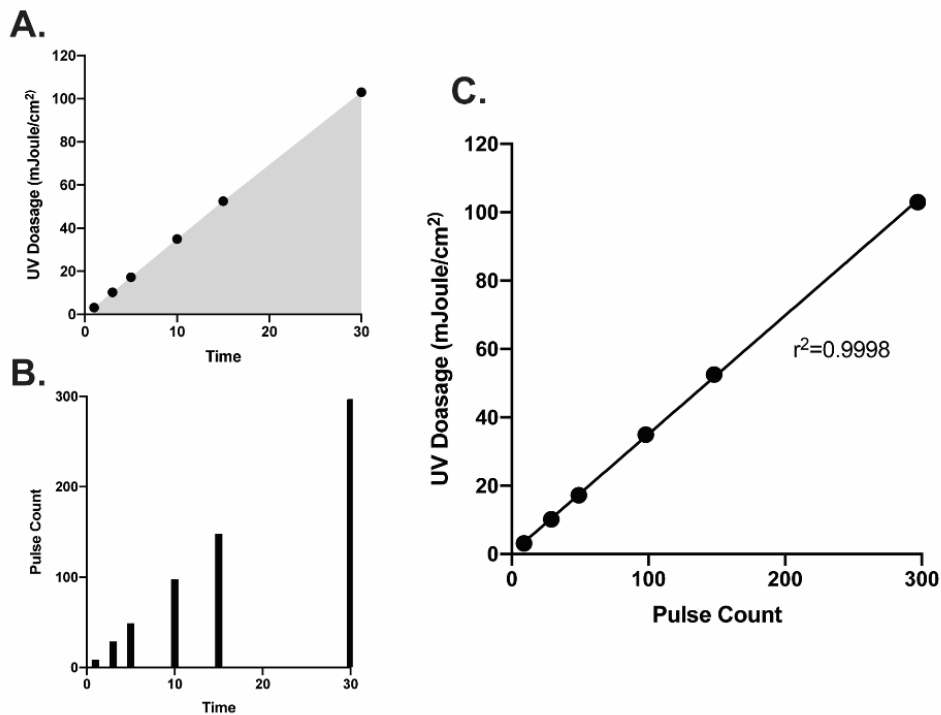
125

## 126 **Results**

### 127 *UV dosage and pulse counts show significant correlation*

128 We first determined the range of UV dosage that could be achieve with the Helo F2 device  
129 between 1 and 30 minutes of exposure. The device produces a theoretical 10 pulses per minute.  
130 In practice, we achieved 6 pulses after 1 minute and 297 pulses after 30 minutes, corresponding  
131 to cumulative UV doses of 3.14 mJ/cm<sup>2</sup> and 103 mJ/cm<sup>2</sup>, respectively (Figure 1A, B). Interestingly,  
132 we observed the UV dosage output by the Helo F2 device over time has a significant and linear  
133 correlation with the overall pulse count (Figure 1C). This suggests that it is possible to identify a  
134 specific amount of time required for inactivation depending on the dosage required. Additionally,  
135 the exposure times and UV dosage range tested in this study encompass previously reported

136 effective UV exposure times and doses for inactivating SARS-CoV-2 with similar UV devices  
137 [31,32].  
138  
139



140 Broad spectrum pulsed UV light effectively inactivates SARS-CoV-2 on multiple surfaces

**Figure 1.** UV dosage (A) and pulse-counts (B) recorded over time from the Helo F2 device. (C) Pulse count plotted versus UV dosage shows a significant positive correlation. Data were fit with a linear regression in GraphPad prism.

141  
142 To determine the effectiveness of the Helo F2 device in inactivating SARS-CoV-2, glass, stainless  
143 steel, plastic, and N95 respirator material inoculated with SARS-CoV-2 (see materials and  
144 methods) were exposed to pulsed UV light for 1, 3, 5, 10, 15, and 30 minutes from a distance of  
145 1 meter. Time zero represents samples that were inoculated, dried and quantified for infectivity  
146 without UV exposure. SARS-CoV-2 titers recovered from the unexposed UV controls indicate that  
147 the drying process resulted in an approximately 3-fold decrease in titers when compared to the

148 same inoculums that had not been dried prior to titration (Figure 2). Additionally, similar amounts  
149 of SARS-CoV-2 were recovered from all surfaces, indicating that the recovery process was  
150 efficient for all tested surfaces.

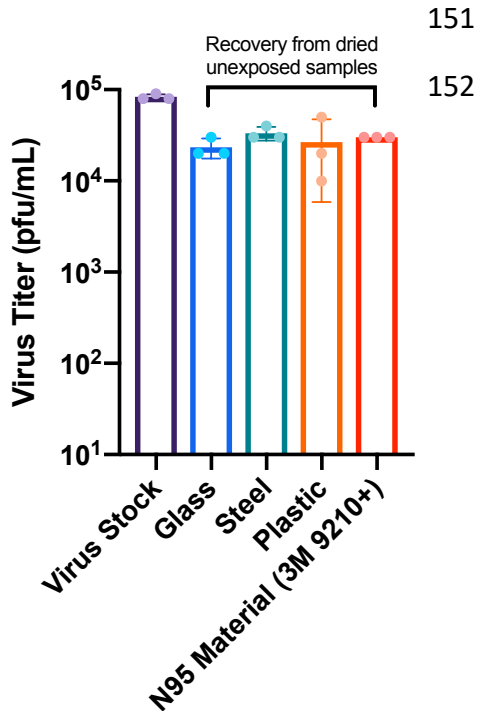


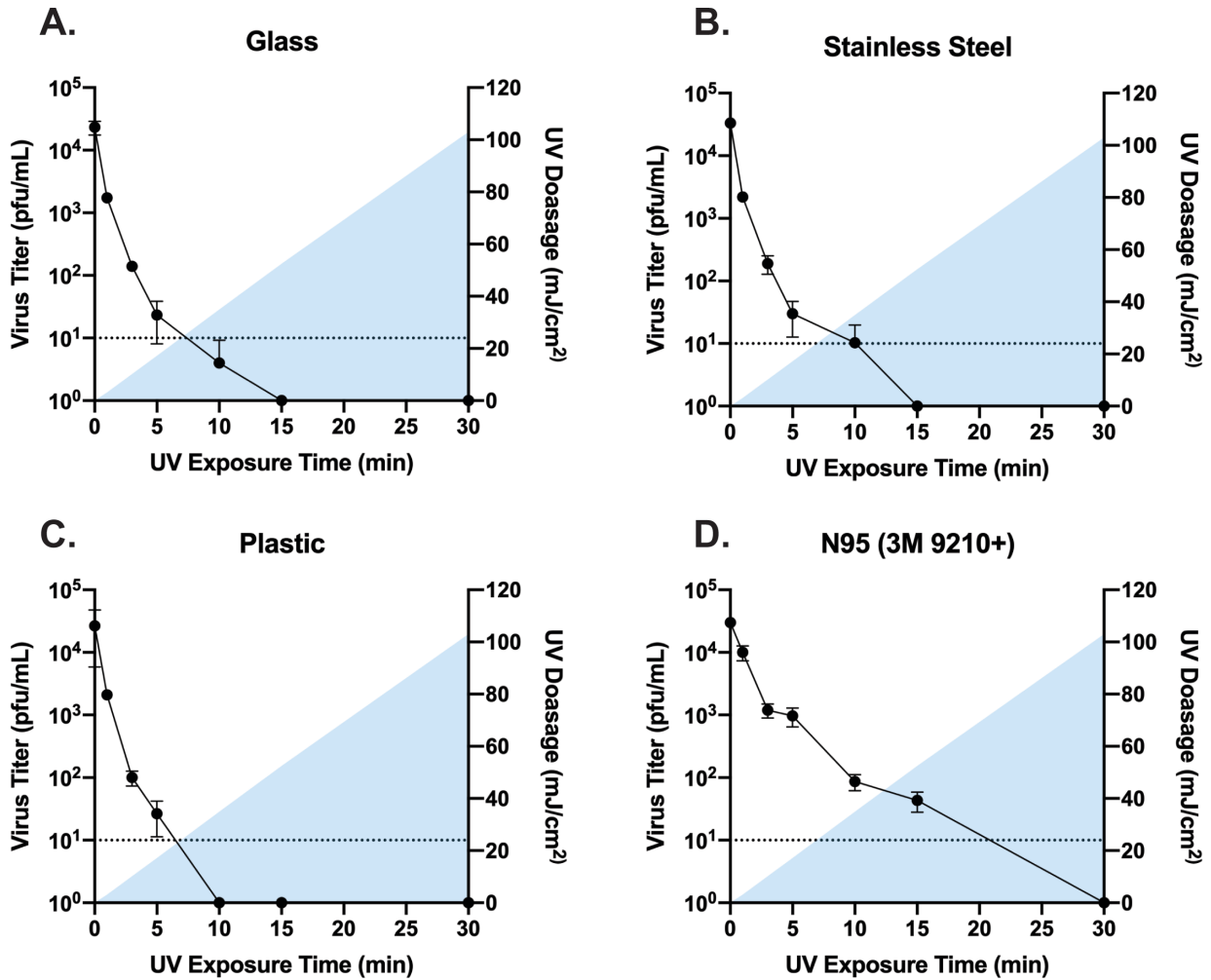
**Figure 2.** Virus titer reduction due to drying. Virus stock represents the amount of virus initially inoculated onto the surfaces. Glass, steel, plastic, and 3M N95 material samples represent the virus titer recovered from dried, unexposed samples after harvesting.

153  
154  
155

156 For the UV exposed samples, we observed that for the hard, non-porous surfaces (glass,  
157 stainless steel, and plastic) a pulse-on time of 5 minutes (17.2 mJ/cm<sup>2</sup>) was sufficient to achieve  
158 a 3-log<sub>10</sub> reduction of infectious virus recovered from the surfaces (Figure 3A-C). Exposure for 10  
159 minutes (34.9 mJ/cm<sup>2</sup>) was sufficient to reduce infectious virus to nearly undetectable levels on  
160 glass and plastic, while 15 minutes (52.5 mJ/cm<sup>2</sup>) was required for the same effect on stainless  
161 steel. N95 respirator material (3M 9210+) required 15 minutes of exposure to achieve a 2.86 log<sub>10</sub>  
162 reduction in infectious virus and 30 minutes (103 mJ/cm<sup>2</sup>) exposure for reduction to undetectable  
163 levels which likely due to the porous and multilayer structure of N95 material (Figure 3D) [33-35].  
164 Taken together, these data suggest that broad-spectrum pulsed UV light is capable of effectively



165 inactivating SARS-CoV-2 in short periods of time on hard non-porous surfaces, and on N95  
166 respirator material with longer exposure times.



167

**Figure 3.** Titers of infectious SARS-CoV-2 recovered from UV exposed glass, stainless steel, plastic, and N95 material (A-D). Time 0 represents controls that were not exposed to UV. All timepoints are representative of the mean and standard error of 3 replicates. Blue shading represents the area under the curve for the UV dosage acquired over time. Samples with data points below the limit of detection resulted from a subset of datapoints having undetectable levels of virus. Undetected samples were assigned a value of 1 for graphing purposes.

168 *Correlating colorimetric UV dosimeter cards to physical UV dosimeter and virus titer reductions.*

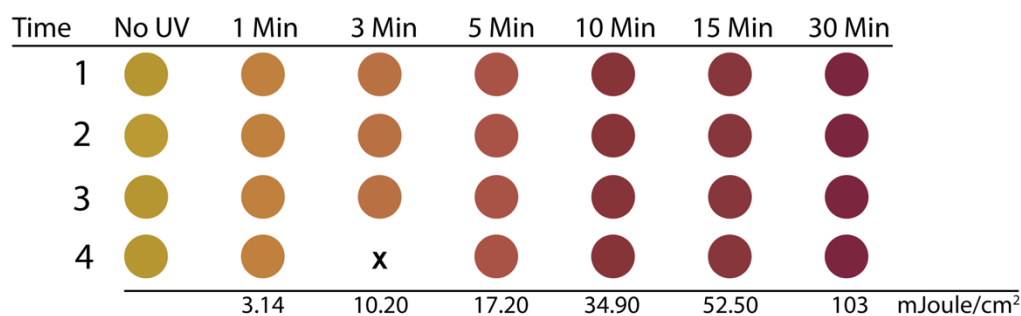
169 From a point-of-use perspective, electronic UV dosimeters like the one employed here are  
170 expensive and require manual set-up and operation, making them a less than ideal option for  
171 ensuring the correct dosage has been applied to a surface. Because of this, UV dosimeter cards  
172 are available that exhibit a colorimetric change in response to increasing doses of UV light. In  
173 tandem with testing the effectiveness of broad-spectrum UV light in inactivating SARS-CoV-2, we  
174 were also interested in determining the functionality of UV dosage cards specifically designed for  
175 pulsed-UV light sources. To test their functionality, 4 test pieces of experimental UV dosage card  
176 material were included in each UV exposure timepoint. We determined that these functioned as  
177 intended with a significant color change occurring with increasing doses of UV (Figure 4A). We  
178 identified that the color change was even across all cards recovered at each timepoint indicating  
179 a high degree of reproducibility across the material (Supplemental Figure 3). Given that these  
180 cards would be intended for end-users to ensure that a high enough dosage had been applied for  
181 inactivation, we compiled our UV dosage meter and SARS-CoV-2 titer reduction data to correlate  
182 with the color change from the cards (Figure 4B). Taken together this UV reactive card material  
183 represents an effective alternative to high-cost dosage meters for end users of broad-spectrum  
184 pulsed UV disinfection equipment.

185

186 **Discussion**

187 The availability of information regarding the inactivation of SARS-CoV-2 for environmental  
188 disinfection is of paramount importance. UV disinfection is a validated technology that has been  
189 utilized for decades to inactivate pathogens on surfaces, as well as in air and water [36,37]. The  
190 effectiveness of UV light, pulsed or constant, in inactivating pathogens is expected to be directly  
191 related to the dosage applied [33]. Here, we have described empirically determined dosages of  
192 broad-spectrum, pulsed UV light that are effective for the inactivation of SARS-CoV-

193



**B.**

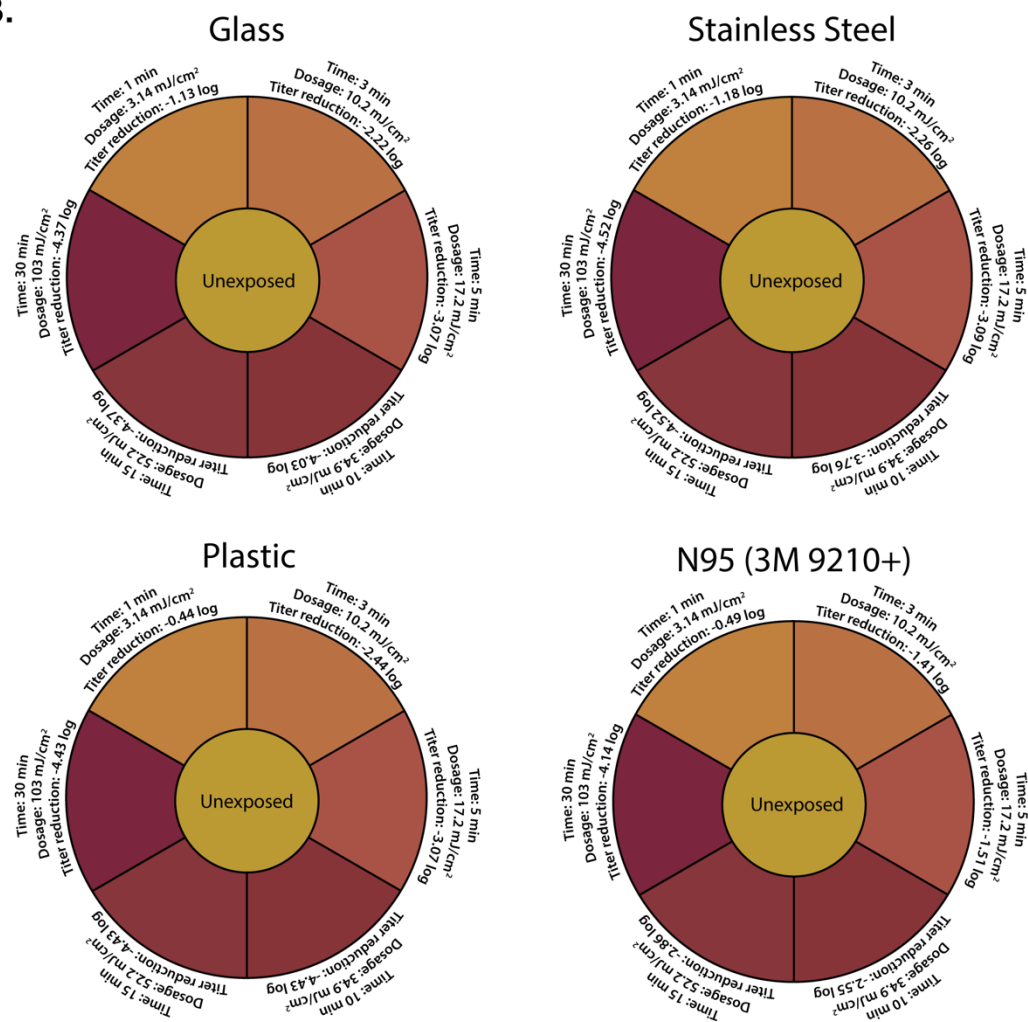


**Figure 5.** (A) Colorimetric change of indicator cards at indicated timepoints and dosages. (B) Compilation of time, dosage, and SARS-CoV-2 titer reduction data as a function of indicator card color. Indicator color in A and B is graphically depicted by using the eyedropper color tool within Adobe Illustrator on recovered UV indicator cards.

195 2 on multiple relevant surfaces. Additionally, we have also demonstrated the effectiveness of  
196 colorimetric UV dosimeter cards for dosage determination by the end-user.

197

198 While only a single device was tested in this study, a variety of UV inactivation studies have been  
199 published focusing on SARS-CoV-2 and other coronaviruses using different wavelengths and  
200 environmental conditions [38-43]. This has led to the development of new UV disinfection products  
201 in an effort to address proper disinfection of PPE and surfaces as the pandemic continues [44].  
202 Disinfection of potentially contaminated surfaces by broad-spectrum UV light is a particularly  
203 attractive option when compared to chemical disinfectants as its less laborious and does not  
204 require close contact with contaminated surfaces. Additionally, with PPE shortages being an  
205 ongoing concern, our data demonstrates that broad-spectrum pulsed UV could be an effective  
206 strategy for the disinfection of N95 respirators, although our study did not determine how pulsed  
207 UV exposure affects N95 performance.

208

209 While our data demonstrate that broad-spectrum pulsed UV light is an effective method for  
210 inactivating SARS-CoV-2, one notable limitation of our study is that surfaces were only exposed  
211 to the UV light at a distance of one meter. However, our data demonstrated that colorimetric UV  
212 dosimeter cards work as expected and provide a clear indication of the dosage being applied to  
213 a particular surface where the card is in place. In the event that a surface is more than one meter  
214 from a given UV device, using our data as a reference the inverse square law could be applied to  
215 determine the amount of time required to achieve a particular dosage at the necessary distance  
216 [45-47]. In addition, utilizing UV dosimeter cards like those tested here would provide a rapid, low-  
217 cost method for testing broad-spectrum pulsed UV light devices at different distances to ensure  
218 that an effective dosage is delivered.

219

220 The data presented here demonstrate that broad-spectrum UV light is an effective means of  
221 inactivating SARS-CoV-2 on multiple surfaces, including N95 respirator material. Additionally, UV  
222 dosimeter cards like those tested here represent an effective and straightforward means for point-  
223 of-care users of UV disinfection equipment to ensure that surfaces have been properly  
224 disinfected.

225 **Acknowledgments and Competing Interests.** We would like to acknowledge the GSU High  
226 Containment Core for their assistance in performing these studies. PURO UV Disinfection  
227 Lighting provided the Puro UV Helo F2 device, the UV dosimeter cards, the UV meter and funds  
228 for the studies described. All data and analyses were collected and performed without input from  
229 PURO UV Disinfection Lighting.

230

## 231 References

232

- 233 1. Zhu, N.; Zhang, D.; Wang, W.; Li, X.; Yang, B.; Song, J.; Zhao, X.; Huang, B.; Shi, W.; Lu,  
234 R., et al. A Novel Coronavirus from Patients with Pneumonia in China, 2019. *N Engl J Med*  
235 **2020**, *382*, 727-733, doi:10.1056/NEJMoa2001017.
- 236 2. Holshue, M.L.; DeBolt, C.; Lindquist, S.; Lofy, K.H.; Wiesman, J.; Bruce, H.; Spitters, C.;  
237 Ericson, K.; Wilkerson, S.; Tural, A., et al. First Case of 2019 Novel Coronavirus in the  
238 United States. *N Engl J Med* **2020**, *382*, 929-936, doi:10.1056/NEJMoa2001191.
- 239 3. Gorbalenya, A.E.; Baker, S.C.; Baric, R.S.; de Groot, R.J.; Drosten, C.; Gulyaeva, A.A.;  
240 Haagmans, B.L.; Lauber, C.; Leontovich, A.M.; Neuman, B.W., et al. The species Severe  
241 acute respiratory syndrome-related coronavirus: classifying 2019-nCoV and naming it  
242 SARS-CoV-2. *Nature Microbiology* **2020**, *5*, 536-544, doi:10.1038/s41564-020-0695-z.
- 243 4. COVID-19 Weekly Epidemiological Update 7 February 2021. *World Health Organization*  
244 **2020**.
- 245 5. van Doremalen, N.; Bushmaker, T.; Morris, D.H.; Holbrook, M.G.; Gamble, A.; Williamson,  
246 B.N.; Tamin, A.; Harcourt, J.L.; Thornburg, N.J.; Gerber, S.I., et al. Aerosol and Surface  
247 Stability of SARS-CoV-2 as Compared with SARS-CoV-1. *N Engl J Med* **2020**, *382*, 1564-  
248 1567, doi:10.1056/NEJMc2004973.
- 249 6. Zhou, J.; Otter, J.A.; Price, J.R.; Cimpeanu, C.; Garcia, D.M.; Kinross, J.; Boshier, P.R.;  
250 Mason, S.; Bolt, F.; Holmes, A.H., et al. Investigating SARS-CoV-2 surface and air  
251 contamination in an acute healthcare setting during the peak of the COVID-19 pandemic  
252 in London. *Clin Infect Dis* **2020**, 10.1093/cid/ciaa905, doi:10.1093/cid/ciaa905.
- 253 7. Santarpia, J.L.; Rivera, D.N.; Herrera, V.L.; Morwitzer, M.J.; Creager, H.M.; Santarpia,  
254 G.W.; Crown, K.K.; Brett-Major, D.M.; Schnaubelt, E.R.; Broadhurst, M.J., et al. Aerosol  
255 and surface contamination of SARS-CoV-2 observed in quarantine and isolation care. *Sci*  
256 *Rep* **2020**, *10*, 12732, doi:10.1038/s41598-020-69286-3.
- 257 8. Ong, S.W.X.; Tan, Y.K.; Chia, P.Y.; Lee, T.H.; Ng, O.T.; Wong, M.S.Y.; Marimuthu, K. Air,  
258 Surface Environmental, and Personal Protective Equipment Contamination by Severe

- 259 Acute Respiratory Syndrome Coronavirus 2 (SARS-CoV-2) From a Symptomatic Patient.  
260 *JAMA* **2020**, 323, 1610-1612, doi:10.1001/jama.2020.3227.
- 261 9. Guo, Z.D.; Wang, Z.Y.; Zhang, S.F.; Li, X.; Li, L.; Li, C.; Cui, Y.; Fu, R.B.; Dong, Y.Z.; Chi,  
262 X.Y., et al. Aerosol and Surface Distribution of Severe Acute Respiratory Syndrome  
263 Coronavirus 2 in Hospital Wards, Wuhan, China, 2020. *Emerg Infect Dis* **2020**, 26, 1583-  
264 1591, doi:10.3201/eid2607.200885.
- 265 10. Colaneri, M.; Seminari, E.; Novati, S.; Asperges, E.; Biscarini, S.; Piralla, A.; Percivalle,  
266 E.; Cassaniti, I.; Baldanti, F.; Bruno, R., et al. Severe acute respiratory syndrome  
267 coronavirus 2 RNA contamination of inanimate surfaces and virus viability in a health care  
268 emergency unit. *Clin Microbiol Infect* **2020**, 26, 1094 e1091-1094 e1095,  
269 doi:10.1016/j.cmi.2020.05.009.
- 270 11. Suzuki, M.; Kamiya, H.; Okamoto, K.; Yamagishi, T.; Kakimoto, K.; Takeda, M.;  
271 Matsuyama, S.; Shirato, K.; Nao, N.; Hasegawa, H., et al. Environmental sampling for  
272 severe acute respiratory syndrome coronavirus 2 (SARS-CoV-2) during a coronavirus  
273 disease (COVID-19) outbreak aboard a commercial cruise ship. *medRxiv* **2020**,  
274 10.1101/2020.05.02.20088567, 2020.2005.2002.20088567,  
275 doi:10.1101/2020.05.02.20088567.
- 276 12. Maestre, J.P.; Jarma, D.; Yu, C.; Siegel, J.; Horner, S.; Kinney, K.A. Distribution of SARS-  
277 CoV-2 RNA Signal in a Home with COVID-19 Positive Occupants. *medRxiv* **2020**,  
278 10.1101/2020.11.30.20234393, 2020.2011.2030.20234393,  
279 doi:10.1101/2020.11.30.20234393.
- 280 13. Döhla, M.; Wilbring, G.; Schulte, B.; Kümmerer, B.M.; Diegmann, C.; Sib, E.; Richter, E.;  
281 Haag, A.; Engelhart, S.; Eis-Hübinger, A.M., et al. SARS-CoV-2 in environmental samples  
282 of quarantined households. *medRxiv* **2020**, 10.1101/2020.05.28.20114041,  
283 2020.2005.2028.20114041, doi:10.1101/2020.05.28.20114041.
- 284 14. World Health, O. *Cleaning and disinfection of environmental surfaces in the context of*  
285 *COVID-19: interim guidance, 15 May 2020*; World Health Organization: Geneva, 2020,  
286 2020.
- 287 15. Paul, D.; Gupta, A.; Maurya, A.K. Exploring options for reprocessing of N95 Filtering  
288 Facepiece Respirators (N95-FFRs) amidst COVID-19 pandemic: A systematic review.  
289 *PLoS One* **2020**, 15, e0242474, doi:10.1371/journal.pone.0242474.
- 290 16. Derraik, J.G.B.; Anderson, W.A.; Connelly, E.A.; Anderson, Y.C. Rapid Review of SARS-  
291 CoV-1 and SARS-CoV-2 Viability, Susceptibility to Treatment, and the Disinfection and  
292 Reuse of PPE, Particularly Filtering Facepiece Respirators. *Int J Environ Res Public*  
293 *Health* **2020**, 17, doi:10.3390/ijerph17176117.
- 294 17. Ma, Q.X.; Shan, H.; Zhang, C.M.; Zhang, H.L.; Li, G.M.; Yang, R.M.; Chen, J.M.  
295 Decontamination of face masks with steam for mask reuse in fighting the pandemic  
296 COVID-19: Experimental supports. *J Med Virol* **2020**, 92, 1971-1974,  
297 doi:10.1002/jmv.25921.
- 298 18. Ibanez-Cervantes, G.; Bravata-Alcantara, J.C.; Najera-Cortes, A.S.; Meneses-Cruz, S.;  
299 Delgado-Balbuena, L.; Cruz-Cruz, C.; Duran-Manuel, E.M.; Cureno-Diaz, M.A.; Gomez-  
300 Zamora, E.; Chavez-Ocana, S., et al. Disinfection of N95 masks artificially contaminated  
301 with SARS-CoV-2 and ESKAPE bacteria using hydrogen peroxide plasma: Impact on the  
302 reutilization of disposable devices. *Am J Infect Control* **2020**, 48, 1037-1041,  
303 doi:10.1016/j.ajic.2020.06.216.
- 304 19. Hamzavi, I.H.; Lyons, A.B.; Kohli, I.; Narla, S.; Parks-Miller, A.; Gelfand, J.M.; Lim, H.W.;  
305 Ozog, D.M. Ultraviolet germicidal irradiation: Possible method for respirator disinfection to  
306 facilitate reuse during the COVID-19 pandemic. *J Am Acad Dermatol* **2020**, 82, 1511-  
307 1512, doi:10.1016/j.jaad.2020.03.085.
- 308 20. Daeschler, S.C.; Manson, N.; Joachim, K.; Chin, A.W.H.; Chan, K.; Chen, P.Z.; Tajdaran,  
309 K.; Mirmoeini, K.; Zhang, J.J.; Maynes, J.T., et al. Effect of moist heat reprocessing of N95



- 310 respirators on SARS-CoV-2 inactivation and respirator function. *CMAJ* **2020**, *192*, E1189-  
311 E1197, doi:10.1503/cmaj.201203.
- 312 21. Chou, R.; Dana, T.; Jungbauer, R.; Weeks, C.; McDonagh, M.S. Masks for Prevention of  
313 Respiratory Virus Infections, Including SARS-CoV-2, in Health Care and Community  
314 Settings : A Living Rapid Review. *Ann Intern Med* **2020**, *173*, 542-555, doi:10.7326/M20-  
315 3213.
- 316 22. Cheng, V.C.C.; Wong, S.C.; Kwan, G.S.W.; Hui, W.T.; Yuen, K.Y. Disinfection of N95  
317 respirators by ionized hydrogen peroxide during pandemic coronavirus disease 2019  
318 (COVID-19) due to SARS-CoV-2. *J Hosp Infect* **2020**, *105*, 358-359,  
319 doi:10.1016/j.jhin.2020.04.003.
- 320 23. Celina, M.C.; Martinez, E.; Omana, M.A.; Sanchez, A.; Wiemann, D.; Tezak, M.;  
321 Dargaville, T.R. Extended use of face masks during the COVID-19 pandemic - Thermal  
322 conditioning and spray-on surface disinfection. *Polym Degrad Stab* **2020**, *179*, 109251,  
323 doi:10.1016/j.polymdegradstab.2020.109251.
- 324 24. Carrillo, I.O.; Floyd, A.C.E.; Valverde, C.M.; Tingle, T.N.; Zabaneh, F.R. Immediate-use  
325 steam sterilization sterilizes N95 masks without mask damage. *Infect Control Hosp*  
326 *Epidemiol* **2020**, *41*, 1104-1105, doi:10.1017/ice.2020.145.
- 327 25. Al-Sayah, M.H. Chemical disinfectants of COVID-19: an overview. *J Water Health* **2020**,  
328 *18*, 843-848, doi:10.2166/wh.2020.108.
- 329 26. Kratzel, A.; Todt, D.; V'kovski, P.; Steiner, S.; Gultom, M.L.; Thao, T.T.N.; Ebert, N.;  
330 Holwerda, M.; Steinmann, J.; Niemeyer, D., et al. Efficient inactivation of SARS-CoV-2 by  
331 WHO-recommended hand rub formulations and alcohols. *bioRxiv* **2020**,  
332 10.1101/2020.03.10.986711, 2020.2003.2010.986711, doi:10.1101/2020.03.10.986711.
- 333 27. Leslie, R.A.; Zhou, S.S.; Macinga, D.R. Inactivation of SARS-CoV-2 by commercially  
334 available alcohol-based hand sanitizers. *Am J Infect Control* **2020**,  
335 10.1016/j.ajic.2020.08.020, doi:10.1016/j.ajic.2020.08.020.
- 336 28. Xiling, G.; Yin, C.; Ling, W.; Xiaosong, W.; Jingjing, F.; Fang, L.; Xiaoyan, Z.; Yiyue, G.;  
337 Ying, C.; Lunbiao, C., et al. In vitro inactivation of SARS-CoV-2 by commonly used  
338 disinfection products and methods. *Sci Rep* **2021**, *11*, 2418, doi:10.1038/s41598-021-  
339 82148-w.
- 340 29. Budowsky, E.I.; Bresler, S.E.; Friedman, E.A.; Zheleznova, N.V. Principles of selective  
341 inactivation of viral genome. I. UV-induced inactivation of influenza virus. *Arch Virol* **1981**,  
342 *68*, 239-247, doi:10.1007/BF01314577.
- 343 30. Jureka, A.S.; Silvas, J.A.; Basler, C.F. Propagation, Inactivation, and Safety Testing of  
344 SARS-CoV-2. *Viruses* **2020**, *12*, doi:10.3390/v12060622.
- 345 31. Kitagawa, H.; Nomura, T.; Nazmul, T.; Omori, K.; Shigemoto, N.; Sakaguchi, T.; Ohge, H.  
346 Effectiveness of 222-nm ultraviolet light on disinfecting SARS-CoV-2 surface  
347 contamination. *Am J Infect Control* **2020**, 10.1016/j.ajic.2020.08.022,  
348 doi:10.1016/j.ajic.2020.08.022.
- 349 32. Simmons, S.E.; Carrion, R.; Alfson, K.J.; Staples, H.M.; Jinadatha, C.; Jarvis, W.R.;  
350 Sampathkumar, P.; Chemaly, R.F.; Khawaja, F.; Povroznik, M., et al. Deactivation of  
351 SARS-CoV-2 with pulsed-xenon ultraviolet light: Implications for environmental COVID-19  
352 control. *Infect Control Hosp Epidemiol* **2020**, 10.1017/ice.2020.399, 1-4,  
353 doi:10.1017/ice.2020.399.
- 354 33. Raeiszadeh, M.; Adeli, B. A Critical Review on Ultraviolet Disinfection Systems against  
355 COVID-19 Outbreak: Applicability, Validation, and Safety Considerations. *Acs Photonics*  
356 **2020**, *7*, 2941-2951, doi:10.1021/acsp Photonics.0c01245.
- 357 34. Cadnum, J.L.; Li, D.F.; Redmond, S.N.; John, A.R.; Pearlmutter, B.; Donskey, C.J.  
358 Effectiveness of Ultraviolet-C Light and a High-Level Disinfection Cabinet for  
359 Decontamination of N95 Respirators. *Pathog Immun* **2020**, *5*, 52-67,  
360 doi:10.20411/pai.v5i1.372.

- 361 35. Mills, D.; Harnish, D.A.; Lawrence, C.; Sandoval-Powers, M.; Heimbuch, B.K. Ultraviolet  
362 germicidal irradiation of influenza-contaminated N95 filtering facepiece respirators. *Am J*  
363 *Infect Control* **2018**, *46*, e49-e55, doi:10.1016/j.ajic.2018.02.018.
- 364 36. Bolton, J.R.; Cotton, C.A. *The ultraviolet disinfection handbook*, 1st ed.; American Water  
365 Works Association: Denver, CO, 2008; pp. xv, 149 p.
- 366 37. Kowalski, W.J. *Ultraviolet germicidal irradiation handbook : UVGI for air and surface*  
367 *disinfection*; Springer-Verlag: Heidelberg ; New York, 2009; pp. xvii, 501 p.
- 368 38. Pendyala, B.; Patras, A.; Pokharel, B.; D'Souza, D. Genomic Modeling as an Approach to  
369 Identify Surrogates for Use in Experimental Validation of SARS-CoV-2 and HuNoV  
370 Inactivation by UV-C Treatment. *Front Microbiol* **2020**, *11*, 572331,  
371 doi:10.3389/fmicb.2020.572331.
- 372 39. Patterson, E.I.; Prince, T.; Anderson, E.R.; Casas-Sanchez, A.; Smith, S.L.; Cansado-  
373 Utrilla, C.; Solomon, T.; Griffiths, M.J.; Acosta-Serrano, A.; Turtle, L., et al. Methods of  
374 Inactivation of SARS-CoV-2 for Downstream Biological Assays. *J Infect Dis* **2020**, *222*,  
375 1462-1467, doi:10.1093/infdis/jiaa507.
- 376 40. Inagaki, H.; Saito, A.; Sugiyama, H.; Okabayashi, T.; Fujimoto, S. Rapid inactivation of  
377 SARS-CoV-2 with deep-UV LED irradiation. *Emerg Microbes Infect* **2020**, *9*, 1744-1747,  
378 doi:10.1080/22221751.2020.1796529.
- 379 41. Buonanno, M.; Welch, D.; Shuryak, I.; Brenner, D.J. Far-UVC light (222 nm) efficiently and  
380 safely inactivates airborne human coronaviruses. *Sci Rep* **2020**, *10*, 10285,  
381 doi:10.1038/s41598-020-67211-2.
- 382 42. Biasin, M.; Bianco, A.; Pareschi, G.; Cavalleri, A.; Cavatorta, C.; Fenizia, C.; Galli, P.;  
383 Lessio, L.; Lualdi, M.; Tombetti, E., et al. UV-C irradiation is highly effective in inactivating  
384 SARS-CoV-2 replication. *medRxiv* **2021**, 10.1101/2020.06.05.20123463,  
385 2020.2006.2005.20123463, doi:10.1101/2020.06.05.20123463.
- 386 43. Simmons, S.; Carrion, R.; Alfson, K.; Staples, H.; Jinadatha, C.; Jarvis, W.;  
387 Sampathkumar, P.; Chemaly, R.F.; Khawaja, F.; Povroznik, M., et al. Disinfection effect  
388 of pulsed xenon ultraviolet irradiation on SARS-CoV-2 and implications for environmental  
389 risk of COVID-19 transmission. *medRxiv* **2020**, 10.1101/2020.05.06.20093658,  
390 2020.2005.2006.20093658, doi:10.1101/2020.05.06.20093658.
- 391 44. Shining a light on COVID-19. *Nature Photonics* **2020**, *14*, 337-337, doi:10.1038/s41566-  
392 020-0650-9.
- 393 45. Bolton, J.R.; Linden, K.G. Standardization of methods for fluence (UV dose) determination  
394 in bench-scale UV experiments. *J Environ Eng-Asce* **2003**, *129*, 209-215,  
395 doi:10.1061/(ASCE)0733-9372(2003)129:3(209).
- 396 46. Harrington, B.J.; Valigosky, M. Monitoring ultraviolet lamps in biological safety cabinets  
397 with cultures of standard bacterial strains on TSA blood agar. *Labmedicine* **2007**, *38*, 165-  
398 168, doi:10.1309/Wa952bxgdr2uqxna.
- 399 47. Lin, C.Y.; Li, C.S. Control effectiveness of ultraviolet germicidal irradiation on bioaerosols.  
400 *Aerosol Sci Tech* **2002**, *36*, 474-478, doi:Doi 10.1080/027868202753571296.
- 401